Weierstraß–Institut
für Angewandte Analysis und Stochastik

im Forschungsverbund Berlin e.V.

Preprint ISSN 0946 – 8633

Excitability of lasers with integrated dispersive reflector

Vasile Tronciu[1,2], Hans-Jürgen Wünsche[3], Klaus R. Schneider[4],

Mindaugas Radziunas[3,4]

submitted: 18th January 2001

[1] University of Durham,
Department of Physics,
Durham DH1 3LE,
United Kingdom,
E-Mail: V.Z.Tronciu@durham.ac.uk

[2] Technical University of Moldova,
Department of Physics,
Stefan cel Mare 168,
Chisinau MD-2004, Moldova
E-Mail: tronciu@mail.utm.md

[3] Humboldt-Universität zu Berlin,
Institut für Physik,
Invalidenstr. 110,
D-10115 Berlin, Germany
E-Mail: wuensche@physik.hu-berlin.de

[4] Weierstraß Institut für Angewandte
Analysis und Stochastik,
Mohrenstraße 39,
10117 Berlin, Germany
E-Mail: schneider@wias-berlin.de
E-Mail: radziunas@wias-berlin.de

Preprint No. 631

Berlin 2001

1991 *Mathematics Subject Classification.* 78A60,34C60.

Key words and phrases. semiconductor laser, excitability, dispersive reflector, optical feedback.

Edited by
Weierstraß–Institut für Angewandte Analysis und Stochastik (WIAS)
Mohrenstraße 39
D — 10117 Berlin
Germany

Fax: + 49 30 2044975
E-Mail (X.400): c=de;a=d400-gw;p=WIAS-BERLIN;s=preprint
E-Mail (Internet): preprint@wias-berlin.de
World Wide Web: http://www.wias-berlin.de/

Abstract

This paper is concerned with the phenomenon of excitability in semiconductor lasers consisting of a DFB section and a passive dispersive reflector (PDR). We assume that the PDR section contains a Bragg grating and (or) a passive Fabry Perot filter guaranteeing a dispersive reflection of the optical field. We investigate a single mode model for PDR lasers and derive conditions under which excitable behavior can be demonstrated. Especially, we show the existence of a threshold, that is, only perturbations above the threshold imply a large excursion from the steady state, and where the response is almost independent of the strength of the perturbation; moreover we establish the existence of a refractory period, i.e., if a second perturbation is applied before the refractory time has passed, then the system does not respond. Finally, we discuss the importance of excitability for the transmission of signals in communication networks.

1 Introduction

The notion of excitability originally comes from biology [6, 12, 11] and chemistry [4, 7]. Using the language of neurobiology [17, 8], excitability can be explained by the all-or-none behavior of neurons: a sub-threshold stimulus only implies a local (i.e. non-propagated) response, a stimulus above the threshold leads to a pulse propagating along the axon.

More recently, excitability has been found also in optical systems such as cavity [9], lasers with saturable absorber [5], and semiconductor laser subjected to delayed optical feedback [10]. Excitability in lasers is of great interest because it offers tremendous prospects for practical applications, primarily for optical switching, clock recovery, pulse reshaping, tunable pulses, and for generating a coherent resonance output pulse in communication networks.

In [9] a nonlinear optical cavity has been investigated. It has been shown that excitability of a ring cavity occurs in a small parameter window close to a bistable operating region. The appearance of excitable behavior can be explained by the interaction of the dynamical effects of nonlinear intracavity field saturation and temperature-dependent field absorption in the medium on two different time scales. The corresponding mathematical model represents a slow-fast system. In [5] it has been demonstrated that a laser with a saturable absorber displays excitability. The system is also of a slow-fast nature and is excitable just before the threshold. It constitutes a simple model for Q-switching in a semiconductor laser. In [10] the evidence of excitability within the Lang-Kobayashi model has been reported.

In this paper we have studied the excitability in a laser with a passive dispersive reflector (PDR). The feedback comes from a Bragg grating. Fig. 1 depicts the

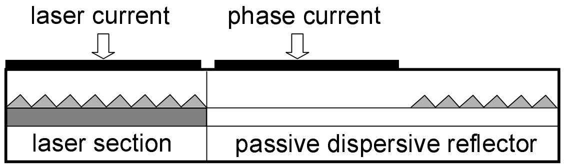

Figure 1: *Schematic illustration of a DFB laser with a passive dispersive reflector.*

structure of the laser, which consists of one active DFB section and a completely passive dispersive reflector. In this model the PDR laser has only one active section to which a pump current is applied. The passive part of the device may consist of different phase and reflector sections or a combination of them. Similar devices are used for generating high frequency self-pulsations (SP) [13], and serve very successful as optical clock in all optical regeneration [14].

In what follows we investigate the single mode approximation of a PDR laser proposed by the authors in Ref [18] in order to determine the parameter regions associated with excitable behavior.

The paper is organized as follows. We present in Section 2 the model equations. In Section 3 we demonstrate excitability in the model of a passive dispersive reflector laser. In section 4 we look for mechanisms producing excitability. To this end we study the phase portrait, discuss possible bifurcations, and make comparison with known excitability scenarios, and establish the existence of pulse trains. Conclusions are given in Section 5.

2 Single mode model

We consider devices in single mode operation. They can be described by single mode rate equations which have already been successfully applied to such devices with an active DFB reflector [2]. For the present case of passive reflectors, only the carrier number N in the laser section and the number S of photons in the total device remain as dynamic variables, and the relevant equations are

$$\frac{dN}{dt} = \frac{I}{e} - \frac{N}{\tau_e} - v_g \Gamma_l g S \; , \qquad \frac{d}{dt}\left(\frac{S}{\sqrt{K_z}}\right) = \left(v_g \Gamma_l g - \gamma_p\right) \frac{S}{\sqrt{K_z}} \; , \tag{2.1}$$

with e being the elementary charge, v_g the group velocity, I the injection current into the laser section and τ_e the spontaneous lifetime. The modal gain g will be used in the simple linear approximation

$$g(N) = g'\,(N - N_{tr})\,,$$

where g' is the differential gain and N_{tr} is the transparency concentration. Furthermore, Γ_l is a *longitudinal* fill factor, i.e., the relative portion of power contained in the laser section. The transverse fill factor is already contained in g', for brevity. γ_p is the optical loss rate, combining the radiation losses at the facets and the internal optical losses. K_z denotes the axial factor of excess spontaneous emission [19]. In devices with multiple sections, the quantities Γ_l, γ_p and K_z are generally functions of the carrier density.

Following the analysis given in [18], it is useful to transform the equations (2.1) into a dimensionless normal form. For these purposes, we introduce dimensionless carrier and photon numbers,

$$n = \frac{N - N_{th}}{N_{th} - N_{tr}} \,, \qquad\qquad p = \frac{\sqrt{K_z^{th}}}{\sqrt{K_z}} \frac{v_g g' \tau_e \Gamma_l^{th}}{N_{th} - N_{tr}} S \,.$$

Here, the threshold carrier number N_{th} is the smallest zero of $(v_g \Gamma_l g - \gamma_p)$. A superscript or subscript th at a N-dependent quantity denotes the value at $N = N_{th}$. With this notation and the dimensionless time $\tau = t/\tau_e$, the desired normal form of the rate equations becomes

$$\frac{dn}{d\tau} = J - n - (1+n)K(n)p \,, \qquad\qquad \frac{dp}{d\tau} = T\,G(n)p \,. \tag{2.2}$$

Here, the parameter $J = (I - I_{th})/(I_{th} - I_{tr})$ denotes the relative excess injection rate, with the threshold current $I_{th} = eN_{th}/\tau_e$ and the transparency current $I_{tr} = eN_{tr}/\tau_e$. Operating the laser sufficiently above threshold, this rate is typically in the range $1 < J < 10$. The parameter $T = \gamma_p^{th}\tau_e$ is the ratio between the carrier and photon life times.

The two rate equation (RE) functions are

$$G(n) = \frac{\Gamma_l(n)}{\Gamma_l^{th}}(1+n) - \frac{\gamma_p(n)}{\gamma_p^{th}} \qquad \text{and} \qquad K(n) = \frac{\Gamma_l(n)}{\Gamma_l^{th}} \sqrt{\frac{K_z(n)}{K_z^{th}}} \,.$$

Without a reflector, i.e., for a solitary DFB laser, it is always the case that $K(n) \equiv 1$ and $G(n) \equiv n$, because Γ_l, K_z and γ_p are independent of n. Some examples can be found in the literature [2, 1, 20] for the carrier density dependence of the quantities Γ_l, γ_p, K_z contained in the RE functions. A narrow resonance-like enhancement of K_z was found as the most prominent feature. This behaviour could be attributed to a nearby point of mode degeneracy at which K_z diverges [20]. Similar results were obtained in [2] for more complicated reflectors composed of a DFB section accomplished by a phase tuning section. We believe that such resonances of K_z due to degeneracy points are a rather general consequence of dispersive reflectors. To study the consequences of these different configurations on the dynamics, we approximate $K(n)$ and $G(n)$ by

$$K(n) = K_0 + \frac{A\,W^2}{4(n - n_0)^2 + W^2} \,, \qquad\qquad G(n) = n + \alpha\,\delta n \,\tanh\left(\frac{n}{\delta n}\right) ,$$

where $A, W, K_0,\ n_0, \alpha, \Delta n$ are parameters. The role of each parameter has been discussed in [18]. In the present study, the majority of parameters is fixed as $J = 2, T = 500, K_0 = 0.5, W = 0.02, A = 10, \alpha = 1, \Delta n = 0.05$. Only the detuning n_0 at which the function $K(n)$ has a resonance peak is varied. Such a variation can be achieved in real devices by tuning the phase current (cf. Fig. 1).

The system described by equations (2.2) has two stationary solutions corresponding to laser "off" and "on". The "on" state is

$$n = 0 \qquad \text{and} \qquad p = \frac{J}{K(0)}. \tag{2.3}$$

which makes sense only for $J > 0$. When varying the detuning n_0 and keeping all other parameters fixed, the resonance structure of K causes a dip of the stationary photon number p as shown in Fig. 2.

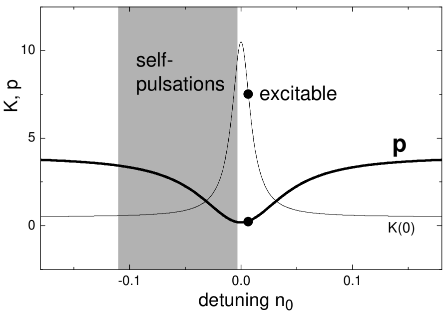

Figure 2: *Dependence of the threshold value* $K(0)$ *(thin solid) and of the stationary reduced photon number* $p = J/K(0)$ *(thick solid) on the detuning parameter* n_0. *The dark region indicates the range of the detuning with self-pulsations. The full dots at* $n_0 = 0.005$ *represent the detuning where excitability is demonstrated in the present work.*

Within a certain range on the left hand side of this dip, the stationary state becomes unstable and self-sustained pulsations emerge. A detailed stability and bifurcation analysis of this phenomenon has been presented elsewhere [18, 3]. On the right hand side of the power depletion, we could find excitability as it will be demonstrated in the next section for the particular detuning $n_0 = 0.005$.

3 Demonstration of excitability

A system is said to be excitable if it shows large excursions from its steady state after applying a short perturbation above some threshold. In particular, such systems exhibit the following properties [9, 5, 10]

(i) There exists a certain threshold such that all perturbations below the threshold imply only small local changes near the steady state.

(ii) To any perturbation above the threshold, the system exhibits a large excursion from its steady state where the shape and size of the response do not depend on the strength of the perturbation.

(iii) After applying a perturbation above the threshold, there is some time interval (refractory period) such that the system is not excitable during that period.

In the present section we domonstrate these features for the particular point of operation described in Fig. 2. For this purpose, we have calculated the response of the system to short perturbations of the injection current.

First, we have applied single rectangular current impulses of variable height δJ_0. The duration $\delta\tau$ of the impulses is as short as $0.025\tau_e$ (25 ps for a typical $\tau_e = 1$ ns life time). Fig. 3 shows two typical reactions of the system. At $\delta J_0 = 0.9$ (left part), the response of the photon number is negligible. Thus, the current pulse can indeed be regarded as a small perturbation. Slightly increasing the perturbation to $\delta J_0 = 1.1$, a much larger excursion of the photon number can be observed (right part of the figure). This behavior is the first indication of excitability.

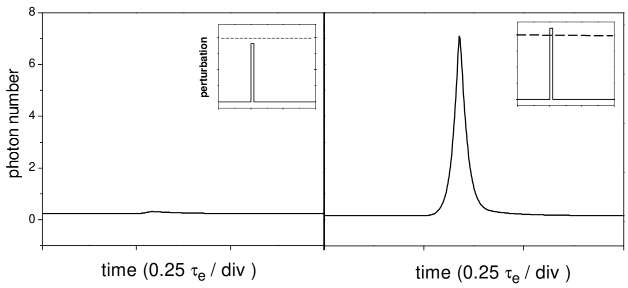

Figure 3: *Calculated transient response to a rectangular current perturbation with $0.025\tau_e$ pulse width. Left part: pulse height $\delta J_0 = 0.9$. Right part: $\delta J_0 = 1.1$.*

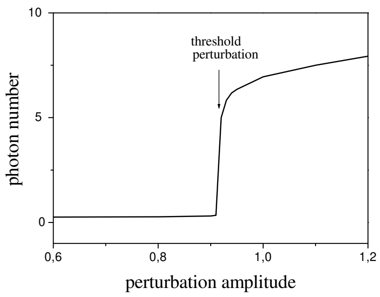

Figure 4: *Dependence of the amplitude p_{max} of the excited pulse on the perturbation amplitude δJ_0.*

The plot of the amplitude p_{max} of the photon pulse versus the perturbation strength δJ_0 gives a clear indication of the existence of a threshold in accordance with the property (i) of excitability (Fig. 4).

Property (ii) is also fulfilled since p_{max} saturates above the threshold.

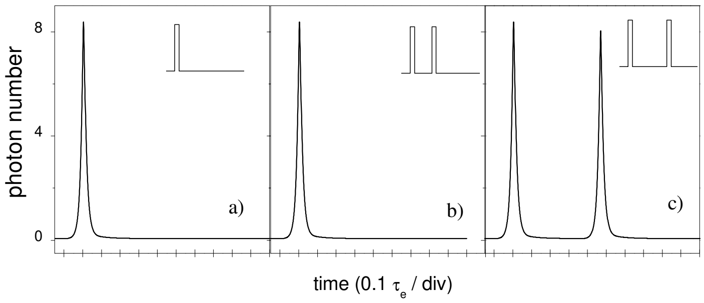

Figure 5: *Response of the system to consecutive current impulses. a) A single impulse for reference. b) Two impulses with $\tau_d = 0.1\tau_e$ delay. c) Two impulses with $\tau_d = 0.4\tau_e$.*

To confirm property (iii) we performed the following numerical simulations. We injected into the system two sequential current impulses above threshold. Fig. 5 b shows the response of the photon number in the case of a small delay between the two pulses (see inset). It does not differ from the response to a single pulse (Fig. 5 a). With a slightly larger delay, however, the two current pulses excite two photon pulses, each one nearly identical to that excited by a single impulse. This is a clear indication of a refractory period which we estimate to be about $0.37\tau_e$ in the present example.

4 Discussion

In the preceding section we have demonstrated excitable behavior of the single mode model for lasers with passive dispersive reflectors. In the present section we shall address in more detail the mechanisms behind this phenomenon, their relations to bifurcations and to known types of excitability, and possible applications.

4.1 Phase space portrait of the observed excitability

Let us assume for the moment that the duration $\delta\tau$ of the applied current impulse is much shorter than the shortest characteristic time of the system. Within this short time, its only effect is to add the amount $\delta n = \delta J_0 \delta\tau$ of carriers to the system by keeping the photon number unchanged at the stationary value p_0. Accordingly, the evolution of the system after the applied impulse follows the phase trajectories starting just at $(n,p) = (\delta n, p_0)$.

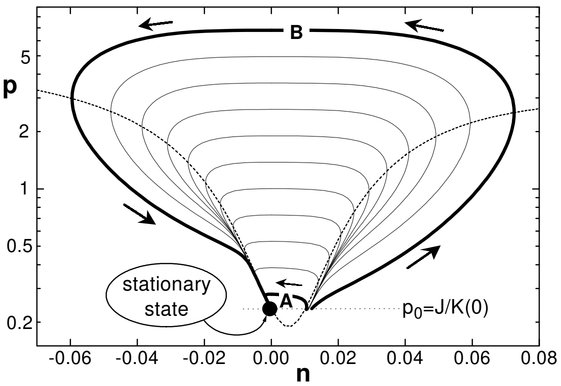

Figure 6: *Trajectories in the (n,p)-phase plane. The detuning is* $n_0 = 0.005$. *The full dot represents the stable stationary state. The drawn trajectories start with the stationary photon number* p_0 *and with excess carrier densities within the small interval between* $n = 0.010$ *and* $n = 0.012$. *The dashed line indicates where the trajectories have a vertical slope.*

Trajectory A belonging to $\delta n = 0.010$ turns immediately to the left approaching the stable node. The maximum $p_{max} = 0.28$ of the photon number during this return is only marginally above the equilibrium value $p_0 = 0.235$. In contrast, trajectory B makes a big loop through a maximum at $p_{max} = 6.9$, although its initial density $n_i = 0.012$ is only a bit larger.

Thus, trajectory A can be denoted as a sub-threshold response, whereas trajectory B represents a super-threshold reponse. In the small interval $p = p_0,\ 0.010 \leq n \leq 0.012$ we have a very sensitive dependence on the initial value. In that case the threshold consists not of a point but of a small interval. Finally, we note that the left boundary point of the threshold interval is very near the curve

$$p_r(n) = \frac{J - n}{(1+n)K(n)} \tag{4.4}$$

where the trajectories have a vertical slope.

To explain this effect we consider the curve corresponding to a function in equation (4.4). In the case of a solitary laser without a dispersive reflector we have $K(n) \equiv 1$, and the function $p_v(n)$ takes approximately the value J. It is a nearly straight line through the stationary point (remember $|n| \ll 1$). It is easy to verify that the stationary point is a stable focus such that all trajectories tend to the focus, and spiral around it. With an appropriate dispersive reflector, $K(n)$ exhibits a strong resonance enhancement that in turn causes a deep minimum of $p_v(n)$ (dashed line in Fig. 6). This implies a slow-fast dynamics near the node. Furthermore, all trajectories of equations (2.2) approach the stable node along a leading direction where this line strongly attracts neighboring trajectories (see Fig. 6). A similar bundling of the phase trajectories can be observed also to the right of the curve (4) near to $p_0 = J/K(0)$. A more detailed analysis of these effect will be presented elsewhere.

4.2 Comparison with know types of excitability

We restrict ourselves to plane vector fields to model excitable systems. In the literature we can find basically two different topological configurations of the trajectories describing excitability: slow-fast systems [6, 11] (see Fig. 7a) and systems where two unstable separatrices of a saddle form a closed curve Γ_0 [5, 15, 16] (see Fig. 7b).

First we consider the saddle case. In Fig. 7b we represent a perturbation by a vertical displacement from the stable steady state. In that case, the threshold corresponds to the distance of the stable separatrix from the steady state. A sub-threshold-perturbation leads only to small local changes. A super-threshold-perturbation leads to a trajectory (it starts at the open circle) going around the closed curve Γ_0 (large excursion).

Next we consider other fast-slow system in Fig. 7a. The motion very near the S-shaped curve is slow where the middle part is repelling and the outer parts attracting. The motion between the S-branches is almost horizontal and fast (jumping behavior). In the left picture we represent a perturbation by a horizontal displacement from the steady state to the right. In that case, the threshold corresponds to the distance of the middle-S branch from the steady state along the horizontal straight line. A sub-threshold perturbation leads to a fast return to the steady state. A super-threshold perturbation (see the open circle) leads first to a jump near the stable right branch, following this branch to the top and then jumping to the left stable branch and following it to the steady state, also a big excursion.

If we compare the phase portraits depictured in Fig. 6 and in Fig. 7, then obviously we have simularities. In the compact region considered there is exactly one steady state which is asymptotically stable and attracts all trajectories. The stationary state is a node with one leading directions where the characteristic numbers are very different. Thus, the trajectories very rapidly approach the leading direction and follow this line slowly such that we can observe a slow-fast behavior near the steady state. On the S-shaped curve in Fig. 7a, the time derivative of the fast variable vanishes; on the dotted line in Fig. 6, the time-derivative of n also vanishes. Both curves have a minimum near the steady state. The nearer in Fig. 6 the steady state is located to the minimum the better we can define the threshold as in the slow-fast system. Far from the steady state in Fig. 6 we cannot distinguish between slow and fast variables. In summary, the phase portraits in Fig. 6 and in Fig. 7a are topologically equivalent, and near the steady state we also represent (2.2) as a fast-slow system.

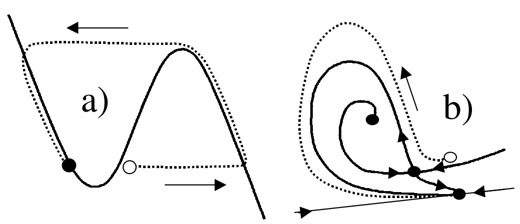

Figure 7: *Schematic phase portraits of different types of excitability in 2D systems. a) Slow-fast system with a S-shaped characteristics like in the FitzHugh-Nagumo model. The horizontal arrows give the direwction of the fast motion. b) Two separatrices of a saddle form a closed curve Γ_0. The steady state is represented by a full circle.*

4.3 Oscillatory behavior

It is well known that excitable systems can also show oscillatory behavior. There are different bifurcations generating a stable limit cycle.

In the case of Fig. 7b a stable large amplitude limit cycle can bifurcate from a homoclinic orbit of a saddle-node when the node coincides with the saddle by changing some parameter.

In the case of Fig. 7a a stable limit cycle can appear by a Hopf bifurcation when the stationary point is slightly shifted through the minimum of the S-shaped curve. In the case of a slow-fast system, the amplitude of the bifurcated limit cycle increases very quickly during a small parameter change (occurence of canard cycles). Our system exhibits the same behavior [18].

It is also interesting to consider the impact of an increasing positiv detuning n_0 on the properties of the excitable system. To this end we compare the phase portrait for the large value $n_0 = 0.025$ depicted in Fig. 9 with that of Fig. 6. The main difference is that the stationary point is shifted upwards on the left slope of the minimum of $p_v(n)$. As a first consequence, its separation from the opposite side of the $p_v(n)$-valley increased. Thus, larger impulses are required to push the system through the valley. Furthermore, this high level of p_0 is above the region where trajectories are closely bundled and the threshold behaviour is more or less lost. We conclude that the excitability phenomenon is most pronounced close to the minimum of $p = p_v(n)$.

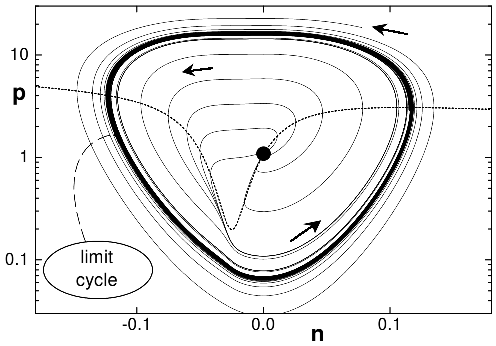

Figure 8: *Phase portrait for* $n_0 = -0.025$. *The dot is the unstable stationary point and the thick solid line represents the stable periodic orbit.*

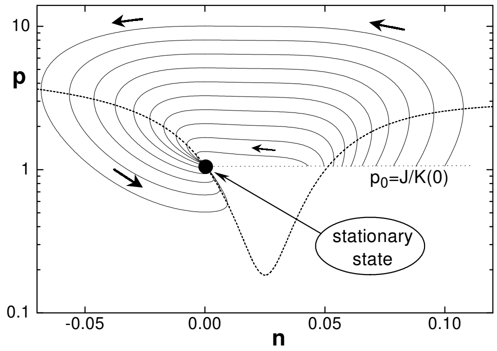

Figure 9: *Phase portrait for* $n_0 = 0.025$. *The depicted phase trajectories start at positions which can be achieved from the stable point (fat dot) by very short current impulses.*

4.4 Possible application of excitability

In the process of transparent optical siganal regeneration the decision element plays a crucial role. It's main function is to distinguish between signals representing noise (0-signals) and signals carrying an information (1-signals).

Let us assume that the 0-signals are small (sub-threshold perturbations) and that the 1-signals have enough power (super-threshold perturbations). The existence of a perturbation threshold in the excitable system (2.2), can be used to suppress the 0-signals and, probably, to equalize 1-signals.

The upper picture of Fig. 10 represents an example of a such incoming pulse train. The dashed line in this picture indicates a threshold of perturbation. The resulting outgoing signal is represented in lower picture of Fig. 10. Only those incoming signals which exceed threshold are able to excite the system (2.2) and are recognized as 1-signals. Other perturbations coursed negligible responce and should be recognized as 0-signals.

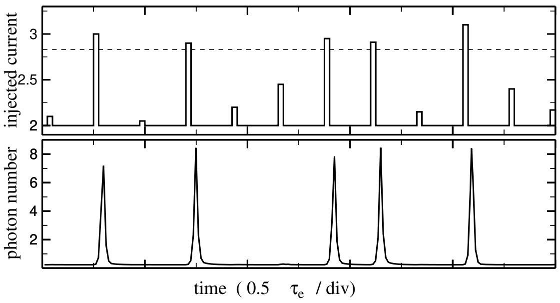

Figure 10: *Response of the system to the train of impulses. The repetition period and impulse length are* $0.45\tau_e$ *and* $0.05\tau_e$, *respectively. Other parameters J=2, A=1, W=0.02,* $K_0 = 0.05$, $\alpha = 1$, $\Delta n = 0.05$, $\tau_e = 1\,ns$. *Small perturbations (noises) are suppressed.*

5 Conclusions

The investigation of a single mode model of a PDR laser exhibits the occurrence of excitability. In the case of a sufficient resonance enhancement of the function $K(n)$, a PDR-laser can be triggered by a small injected current impulse to produce a large excursion from the steady state. A detailed analysis confirmed the existence of a threshold and of a refractory period, and that shape and size of the response are essentially independent of the magnitude of the perturbation. The results obtained confirm the existence of excitable behavior of PDR laser. Practical realization of excitability for PDR lasers remain a subject for future study. However, the results obtained make clear the importance of such work.

Acknowledgments V.Tronciu acknowledges financial support from WIAS, Royal Society NATO Fellowship Programe and Alexander von Humboldt Foundation. V.T. express his gratitude for the hospitality in the group of Prof. Richard Abram at Durham University UK and in the group of Dr. Klaus Schneider at WIAS. We would like to thank Richard Abram for a careful reading of the manuscript.

References

[1] U. Bandelow, H.-J. Wünsche, and H. Wenzel, "Theory of self-pulsations in two-section DFB lasers", *IEEE Photon. Technol. Lett.* **5**, p. 1176 (1993).

[2] U. Bandelow, H.-J. Wünsche, B. Sartorius, and M. Möhrle, "Dispersive self Q-switching in DFB-lasers: theory versus experiment", *IEEE Journal of Selected Topics in Quantum Electronics* **3**, p. 270 (1997).

[3] U. Bandelow, M. Radziunas, V. Tronciu, H.-J. Wünsche, and F. Henneberger, "Tailoring the dynamics of diode lasers by dispersive reflectors", *SPIE Proceedings Series* **3944**, p. 536, (2000).

[4] E. Brink, D.W.U. Bronk, and M.G. Larrabee, "Chemical excitation of nerve", *Ann. New. York Aca. Sci.* **47**, p. 457, (1946).

[5] J.L.A. Dubbeldam, B. Krauskopf, and D. Lenstra, "Excitability and coherence resonance in laser with saturable absorber", *Physical Review E* **60(6)**, p. 6580, (1999).

[6] R. FitzHugh, "Mathematical Models of Threshold Phenomena in the Nerve Membrane", *Bulletine of Mathematical Biophysics* **17**, p. 257, (1955).

[7] S. Grill, V.S. Zykov, and S.C. Müller, "Spiral wave dynamics under pulsatory modulation of excitability", *J. Phys. Chem.* **100** p. 19082, (1996).

[8] E.M. Izhikevich, "Neural Excitability, Spiking, and Bursting", *International J. of Bifurcation and Chaos* **10**, p. 1171, (2000).

[9] W. Lu, D. Yu, and R.G. Harrison, "Excitability in a nonlinear optical cavity", *Phys. Rev. A* **58(2)**, p. 809, (1998).

[10] J. Mulet and C.R. Mirasso, "Numerical statistics of power dropouts based on the Lang-Kobayashi model", *Phys. Rev E* **59(5)**, p. 540, (1999).

[11] J.D. Murray, "Mathematical Biology ", *Springer*, (1990).

[12] J. Rinzel, and G.B. Ermentrout, "Analysis of Neural Excitability and Oscillations", *in C. Koch, I. Segev (eds) Methods in Neuronal Modeling, The MIT Press, Cambridge, Mass.*, (1989).

[13] B. Sartorius, M. Möhrle, S. Reichenbacher, and W. Ebert, "Controllable self-pulsations in multisection DFB lasers with an integrated phase-tuning section" , *IEEE Photon. Technol. Lett.* **7**, p. 1261, (1995).

[14] B. Sartorius, C. Bornholdt, O. Brox, H.J. Ehrke, D. Hoffmann, R. Ludwig, and M. Möhrle, "All-Optical Clock Recovery Module Based on a Self-Pulsating DFB Laser", *Electron. Lett.* **34**, p. 1664, (1998).

[15] K. Schneider, "Über ein mathematisches Modell zur Darstellung von Erregungserscheinungen", *Monatsber. DAW 7*, p. 671-678, (1965).

[16] K. Schneider, "On a model for the kinetics of potassium ions in the membrane of a neuron", *Models of neuronal structures. Nauka, Moscow*, p. 162, (1970).

[17] G.M. Shepherd, "Neurobiology", *Oxford University Press, New York*, (1983).

[18] V.Z. Tronciu, H.-J. Wünsche, J. Sieber, K. Schneider, F. Henneberger, "Dynamics of Single Mode Semiconductor Lasers with Passive Dispersive Reflectors", *Optics Communcations* **182**, p. 221, (2000).

[19] J. Wang, N. Schunk, and K. Petermann, "Linewidth enhancement for DFB lasers due to longitudinal field dependance in the laser cavity", *Electron. Lett.* **23**, p. 715, (1987).

[20] H. Wenzel, U. Bandelow, H.-J. Wünsche, and J. Rehberg, "Mechanisms of fast self pulsations in two-section DFB lasers" , *IEEE J. of Quantum Electronics* **32**, p. 69, (1996).